Synthesis, Structure, and Hydroboration Reactivity of Anionic Nickel(0) Complexes Supported by Bidentate NHC-Pyridone Ligands

Medina Afandiyeva†, Abhishek A. Kadam†, Xijue Wu†, William W. Brennessel, C. Rose Kennedy*

Department of Chemistry, University of Rochester, Rochester, NY 14627, USA

Supporting Information Placeholder

ABSTRACT: A family of anionic, formally nickel(0) complexes supported by bidentate NHC–pyridone ligands is described. The unsymmetric chelating environment and capping $[K(18\text{-crown-6})]^+$ countercation allow isolation of single-component, monometallic complexes in high yield. The steric and electronic properties are assessed through a battery of experimental (NMR, IR, UV/vis, X-ray diffraction) and computational tools. Catalytic activity for highly branched-selective hydroboration of styrene with HBpin is demonstrated. Control experiments implicate an important role of the pyridone in establishing reactivity and regioselectivity, suggesting the potential to leverage secondary coordination sphere effects with these single-component precatalysts for reagent activation and delivery.

INTRODUCTION

N-Heterocyclic carbenes (NHCs) have gained broad popularity in the field of organometallic chemistry since their introduction by Arduengo in 1993.[1, 2] Their ability to coordinate to transition metals through strong σ donation makes them outstanding supporting ligands in numerous contexts. Additionally, modular changes to the core heterocycle composition and/or wingtip substituents offer a suite of electronically and sterically diverse ligand architectures. Recent decades have witnessed extensive development of transition-metal-NHC complexes and their applications in catalysis.[3, 4] In this domain, NHC-supported first-row transition-metals are attractive in comparison to their second- and third-row congeners due to their lower cost, greater availability, and oftentimes unique reactivity profiles.[3, 5-7] In particular, nickel complexes supported by symmetric, monodentate NHCs (e.g. IPr, SIPr, and IMes) have emerged as popular alternatives to Pd-phosphine systems for olefin functionalization,[8, 9] cross coupling,[10, 11] and related reactions (Scheme 1A).

Taking advantage of the modular NHC platform, multidentate NHC derivatives have been developed.[12-14] Commonly these consist of multiple, symmetrically linked NHC units. However, NHC-pyridine, NHC-phosphine, and NHC-amine substructures (among others) have also been introduced.[12-14] These mixed-donor ligands offer an unsymmetric coordination environment and thus can meet distinct electronic and steric needs over the course of a catalytic cycle. Given the versatility of unsymmetric, multidentate NHC ligands, we sought to use the NHC core to develop mixed, bidentate scaffolds with 2-pyridone co-ligands.

Scheme 1. Prior work and motivation for NHC-pyridone design.[a]

A. NHCs as strong σ-donor ligands for [Ni] Catalysis

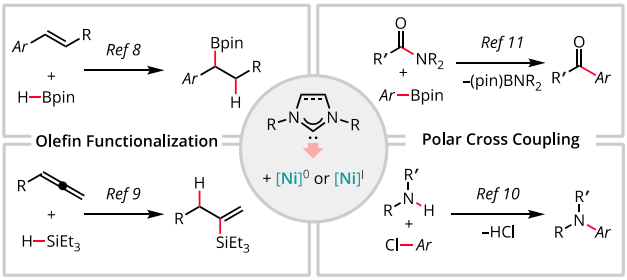

B. Coordination modes of anionic 2-pyridone ligands

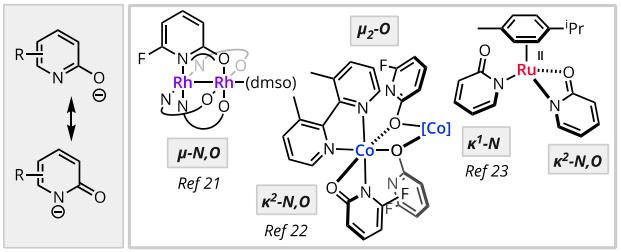

C. This Work: $[Ni]^0$ precatalysts with NHC–pyridone ligands

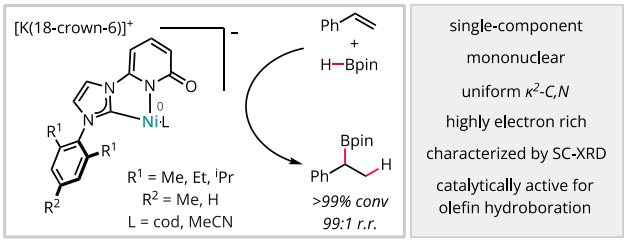

[a] Bpin = pinacolboryl = 4,4,5,5-tetramethyl-1,3-dioxaboryl; dmso = dimethyl sulfoxide; cod = 1,5-cyclooctadiene

Our interest in multidentate pyridone ligands arose due to their tautomeric properties, which suggest possible secondary coordination sphere effects or metal–ligand cooperative reactivity.[15-19] However, 2-pyridone ligands often induce complex speciation with varied μ-N,O, μ-O, κ^1-N, κ^1-O, and/or κ^2-N,O coordination modes (Scheme 1B).[20-23] With group 6–11 metals, this versatile coordination has been shown to promote formation of multimetallic clusters.[20, 21] In pursuit of single-component, mononuclear complexes, we envisioned that a strong co-ligand (such as an NHC) could instead favor a κ^2-C,N coordination geometry with exclusive N-coordination of the pyridone motif.

Herein we report the synthesis and characterization of a family of mononuclear, anionic, formally Ni(0) complexes supported by bidentate NHC-pyridone (C,N) ligands (Scheme 1C). These C,N ligands include ^{h}IMesPyO (1-(2,4,6-trimethylphenyl)-3-(6-oxidopyridin-2-yl)-imidazol-2-ylidene), ^{h}IEtPyO (1-(2,6-diethylphenyl)-3-(6-oxidopyridin-2-yl)-imidazol-2-ylidene), and ^{h}IPrPyO (1-(2,6-diisopropylphenyl)-3-(6-oxidopyridin-2-yl)-imidazol-2-ylidene). Note that the ligand shorthand is adapted from standard conventions for symmetric NHCs (i.e. ^{h}IMes = half-IMes; ^{h}IEt = half-IEt; ^{h}IPr = half-IPr).[2] Although an analogous 3-pyridone ligand has been utilized previously in combination with Ni(II) sources,[24] no structural insights were obtained with catalytically relevant, low-valent nickel. In contrast, the [K(18-crown-6)][(C,N)Ni(L)] (where L = η^2,η^2-1,5-cyclooctadiene or η^2-MeCN) complexes described herein are characterized by NMR, IR, and UV/vis spectroscopies; single-crystal X-ray diffraction analysis (SC-XRD); and computational modeling using density functional theory (DFT). The reactivity of these formally Ni(0) species is benchmarked for hydroboration of styrene with 4,4,5,5-tetramethyl-1,3,2-dioxaborolane (HBpin). Control experiments and stoichiometric studies with HBpin and $B(OMe)_3$ support secondary coordination sphere participation. Taken together, this work demonstrates an effective synthetic strategy for accessing mononuclear Ni-pyridone complexes, elucidates their structural and reactivity features, and shows promise for their application as single-component precatalysts.[6]

RESULTS AND DISCUSSION

Ligand Synthesis. We began our studies with the synthesis of NHC-pyridone ligands by nucleophilic aromatic substitution of 6-chloro-2-hydroxypyridine with *N*-arylimidazoles **1a**–**1c**, which were accessed from the corresponding anilines in a single step (Scheme 2). This approach mirrors that developed previously for NHC-pyridine ligands,[25] and the electrophile was selected on the basis of commercial availability. After trituration, the neat S_NAr reaction yielded imidazolium salts **2a**–**2c** in 42–67% yields. The corresponding free carbenes were obtained following treatment with a strong base (Scheme 2). Initial attempts to access the free carbenes using potassium hexamethyldisilazide (KHMDS) or potassium hydride (KH) led to low purity and/or inconsistent yields of the desired product. However, stirring ^{h}IMesPyOH•HCl (**2a**) with potassium *tert*-butoxide (KO^{t}Bu, 2 equiv.) in toluene at room temperature afforded K[^{h}IMesPyO] in 92% yield. Similarly, K[^{h}IEtPyO] (98% yield) and K[^{h}IPrPyO] (93% yield) were obtained from **2b** and **2c**, respectively. To improve solubility, the potassium salts were complexed with 1 equiv. of 18-crown-6 prior to ^{1}H NMR analysis.

Scheme 2. Synthesis of Free Carbenes 3a–3c

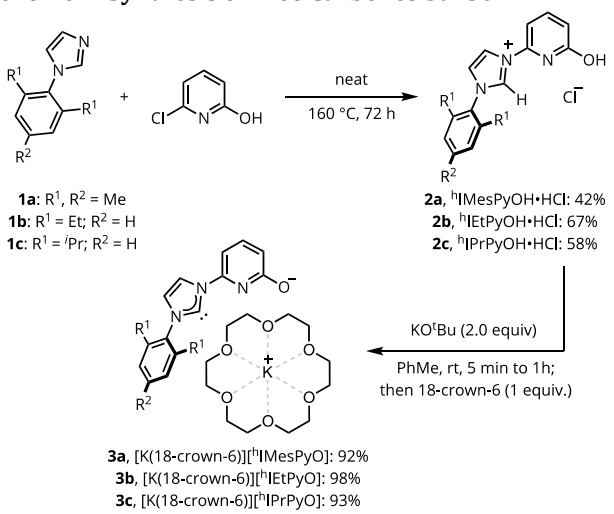

1a: R^1, R^2 = Me
1b: R^1 = Et; R^2 = H
1c: R^1 = ^{i}Pr; R^2 = H

2a, ^{h}IMesPyOH•HCl: 42%
2b, ^{h}IEtPyOH•HCl: 67%
2c, ^{h}IPrPyOH•HCl: 58%

3a, [K(18-crown-6)][^{h}IMesPyO]: 92%
3b, [K(18-crown-6)][^{h}IEtPyO]: 98%
3c, [K(18-crown-6)][^{h}IPrPyO]: 93%

Synthesis of Anionic Nickel (0) Complexes. Metallation of the NHC-pyridone ligands was investigated using [Ni(cod)$_2$], a commercially available Ni(0) source (Scheme 3). At the outset, we treated [Ni(cod)$_2$] with 1 equiv. of [K(18-crown-6)][^{h}IMesPyO] (**3a**) in toluene. Although a color change from sienna brown to dahlia purple was observed within minutes, significant [Ni(cod)$_2$] remained in the crude material (as observed by ^{1}H NMR spectroscopy), even after prolonged stirring at room temperature. Under these conditions, the residual [Ni(cod)$_2$] proved challenging to separate. Incomplete metalation of [Ni(cod)$_2$] is common with monodentate NHC ligands unless the cod is consumed concurrently.[26, 27] Presumably the low equilibrium conversion observed with 1:1 **3a** : [Ni(cod)$_2$] resulted in part from the ligand's low solubility and tight ion pairing with K^+.

Scheme 3. Synthesis of [Ni] Complexes 4a–c and 5a–c

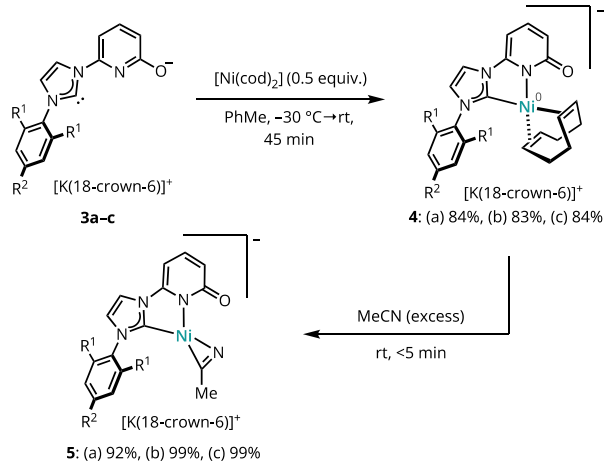

3a–c

4: (a) 84%, (b) 83%, (c) 84%

5: (a) 92%, (b) 99%, (c) 99%

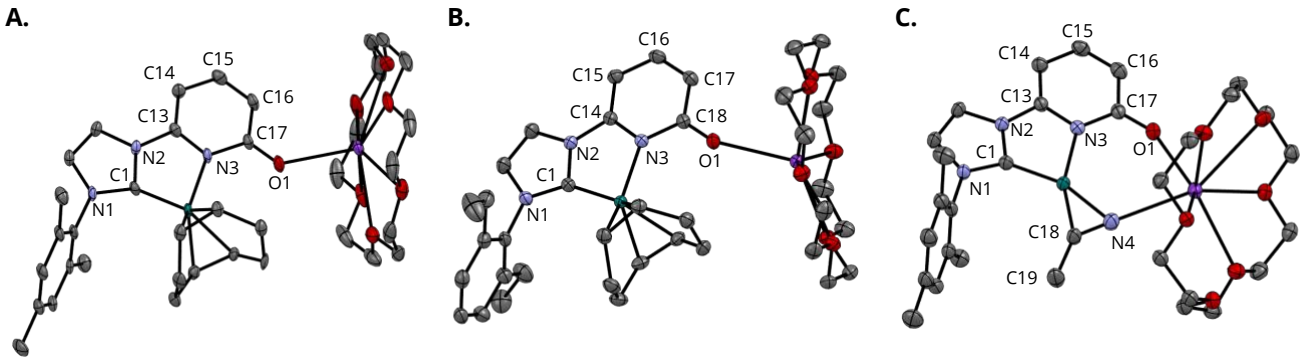

Figure 1. Solid-phase structures of (A) **4a**, (B) **4b**, and (C) **5a** determined by SC-XRD. Thermal ellipsoids depicted at 50% probability. H-atoms and co-crystallized solvent molecules omitted for clarity. C = charcoal, N = blue, O = red, Ni = teal, K = purple

Table 1. Key metrics for the solid-phase structures of 4a, 4b, and 5a determined by SC-XRD.

Bond lengths (Å)				Bond and dihedral angles (°)			
	4a	**4b**	**5a**		**4a**	**4b**	**5a**
Ni(1)-N(3)	2.036(3)	2.0282(11)	2.0361(13)	C(1)-Ni(1)-N(3)	82.34(12)	82.52(5)	82.49(6)
Ni(1)-C(1)	1.873(3)	1.8777(14)	1.8520(16)	C(17)-O(1)-K(1)	132.2(2)	146.85(9)[a]	150.83(11)
K(1)-O(1)	2.586(2)	2.5897(10)	2.5952(13)	C(13)-N(3)-C(17)	118.1(3)	117.99(11)[a]	118.22(13)
O(1)-C(17)	1.256(4)	1.2592(18)[a]	1.255(2)	N(1)-C(1)-N(2)	101.4(3)	101.92(11)	103.03(13)
N(3)-C(13)	1.346(4)	1.3527(18)[a]	1.352(2)	N(3)-C(13)-C(14)	126.2(3)	126.04(13)[a]	126.11(15)
N(3)-C(17)	1.395(4)	1.3934(17)[a]	1.387(2)	C(13)-C(14)-C(15)	116.2(3)	116.05(13)[a]	116.19(15)
C(13)-C(14)	1.383(5)	1.3831(19)[a]	1.376(2)	C(14)-C(15)-C(16)	120.4(3)	120.66(13)[a]	120.30(15)
C(14)-C(15)	1.392(5)	1.396(2)[a]	1.405(2)	C(15)-C(16)-C(17)	121.7(3)	121.26(13)[a]	121.40(15)
C(15)-C(16)	1.363(5)	1.367(2)[a]	1.360(2)	C(1)-N(2)-C(13)-N(3)	-4.7(4)	-0.16(18)[a]	0.6(2)
C(16)-C(17)	1.436(5)	1.4336(19)[a]	1.442(2)	C(1)-N(2)-C(13)-C(14)	175.7(3)	177.97(13)[a]	-178.92(15)
Ni(1)-N(4)	--	--	1.9271(15)	C(18)-N(4)-K(1)	--	--	174.07(13)
Ni(1)-C(18)	--	--	1.8158(16)	N(4)-C(18)-C(19)	--	--	136.31(16)
K(1)-N(4)	--	--	2.7210(15)	N(3)-Ni(1)-C(18)-N(4)	--	--	13.4(2)
N(4)-C(18)	--	--	1.235(2)	C(1)-Ni(1)-C(18)-N(4)	--	--	-177.28(11)
C(18)-C(19)	--	--	1.494(2)	C(1)-Ni(1)-C(18)-C(19)	--	--	4.8(3)

[a] Pyridone C atom index is +1 relative to listed value.

Fortunately, increasing the ligand : $[Ni(cod)_2]$ ratio to 2:1 resulted in a near-complete consumption of $[Ni(cod)_2]$. This approach thus enabled access to [K(18-crown-6)][(^{h}IMesPyO)Ni(cod)] (**4a**) with improved purity and isolated yield (84% yield with respect to [Ni], black cherry solid). Similarly, **3b** and **3c** reacted with $[Ni(cod)_2]$ to form complexes **4b** (83% yield, black grape solid) and **4c** (84% yield, black cherry solid), respectively. Complexes **4a**–**4c** were characterized by ^{1}H and ^{13}C NMR spectroscopy. Single-crystal X-ray diffraction (SC-XRD) data were obtained for **4a** and **4b** (Figure 1).

Due to the strong donating ability of the anionic C,N-ligands, the cod ligands in **4a**–**4c** proved to be labile and underwent facile ligand exchange in the presence of acetonitrile (Scheme 3). The resulting, 3-coordinate,[28-31] 16-electron complexes, **5a**–**5c**, were accessed in ≥92% isolated yield and characterized by ^{1}H and ^{13}C NMR spectroscopy. Single-crystal X-ray diffraction (SC-XRD) data were obtained for **5a**, providing a structural argument for the unexpected stability of the 3-coordinate system (Figure 1, vide infra). These complexes offer (a) improved solubility (compared to **4a**–**4c**) in nonpolar organic solvents and (b) an unsaturated coordination environment suitable for rapid precatalyst activation.

Structural and Spectroscopic Features. Key metrics obtained from single-crystal X-ray diffraction analysis of **4a**, **4b**, and **5a** (Figure 1) are summarized in Table 1. Across the series, consistent κ^2-C,N coordination of the NHC-pyridone ligand was observed with a bite angle of 82–83° and a dihedral angle approaching 0°, indicating high ligand planarity. The heterocyclic C–N, C–C, and C=O bond lengths are most consistent with the pyridone (double bond C=O) resonance description rather than the oxidopyridine (single bond C–O) form.[17, 19, 20] The $[K(18\text{-crown-6})]^+$ counterion was found in a contact ion pair with the pyridone O. We postulate that this ion-pairing interaction caps the pyridone O to prevent bridging coordination modes and multimetallic aggregation. Nonetheless, the steric environment established by the NHC's flanking aryl substituent dominates the environment around [Ni], with little contribution from the $[K(18\text{-crown-6})]^+$ counterion. This is highlighted in a topological steric map of **4a** (Figure

2), where the buried volume (%V_{bur}) in a 3.5 Å sphere is 43.4% for [^{h}IMesPyO]$^{-}$ alone and 43.8% considering the full [K(18-crown-6)][^{h}IMesPyO] ion pair.[32]

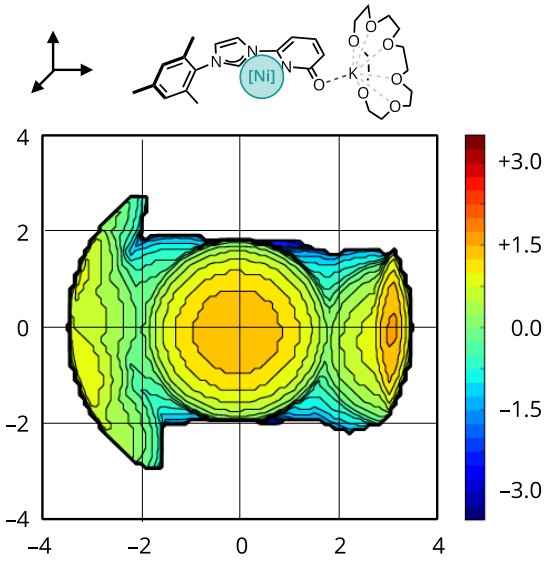

Figure 2. Topological steric map of the [(^{h}IMesPyO)Ni][K(18-crown-6)] coordination sphere obtained from the solid-phase structure of **4a**. Units in Å. Generated with the SambVca 2.1 web app.[32]

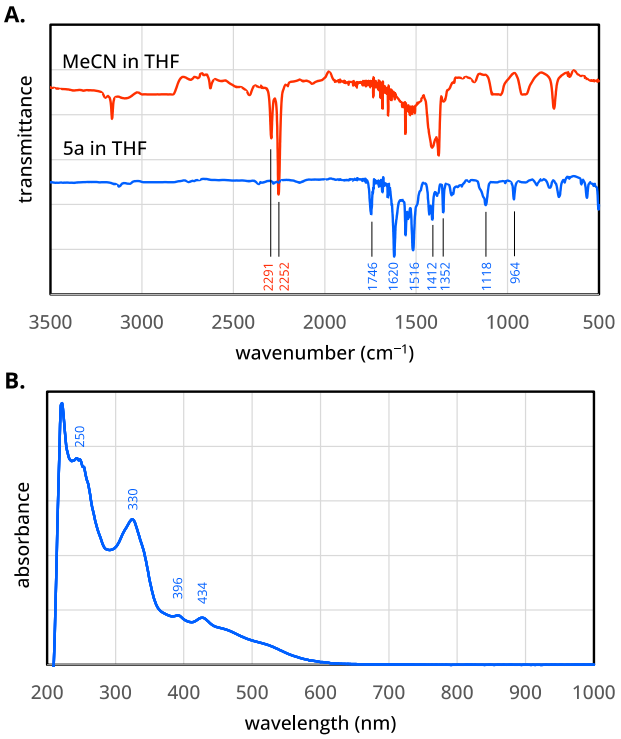

Figure 3. (A) Infrared (IR) and (B) UV/vis absorption features of η^2-MeCN complex **5a**. Measured in THF solution at 25 °C.

Further analysis of the solid-state structure of **5a** revealed unusual η^2 coordination of the nitrile π system with secondary interactions between the acetonitrile N and capping [K(18-crown-6)]$^{+}$ countercation (Figure 1).[33-38] Analysis of the CN bond length (1.235(2) Å) and CCN bond angle (136.31(16)°) indicates substantial π-backbonding from the electron-rich nickel center (Table 1). As such, the formally Ni(0) center is best described as Ni(II) with a 2-electron-reduced nitrile ligand. This assessment is supported by the low CN vibrational frequencies (1746, 964 cm^{-1}, assigned using DFT, Figure 3A) observed by solution-phase infrared spectroscopy of **5a** in THF (vs 2250 cm^{-1} for free MeCN).[39, 40]

The electronic properties of **4a** and **5a** were compared using DFT (B3LYP/def2-TZVP/SMD(THF)) analysis,[41-46] using coordinates from the solid-state structures obtained experimentally. Partial delocalization of anionic character was observed across both the pyridone and π-accepting cod or MeCN ligand (Figure 4A/B). The absolute magnitude of both positive and negative charge accumulation was only slightly greater for **4a** as quantified by the natural charge range (**4a**: −0.76816 (O1) to +0.90053 (K); **5a**: −0.75823 (O1) to +0.89629 (K)) determined through natural population analysis.[46, 47] However, **4a** demonstrated significantly more negative natural charge at Ni (**4a**: −0.16937; **5a**: +0.03488). By contrast, **5a** showed greater overall concentration of negative charge at the pyridone O and delocalization into the nitrile π system.

Optimization from the solid-state structure of **5a** induced little overall change in geometry, bond lengths, or natural charges. Examination of the frontier molecular orbitals (Figure 4C) revealed extensive pyridone π donation into the Ni d_{xz} orbital along with π backbonding into the nitrile ligand (π: HOMO−4; π*: HOMO). Given the high degree of ligand–metal orbital mixing in the frontier molecular orbitals, charge transfer absorption features were expected. Time-dependent DFT analysis was employed to predict the electronic absorption features for comparison with the spectrum collected experimentally (Figure 3b). The absorption features at 434 nm (predicted 432 nm; 58% HOMO−3 to LUMO), 396 nm (predicted 408 nm; 55% HOMO to LUMO), and 330 nm (predicted 321 nm; 93% HOMO−4 to LUMO) all demonstrated significant metal-to-ligand charge-transfer (MLCT) character with d to π*-like transitions. These absorption patterns further underscore both the high degree of charge delocalization and the electronic ambiguity of the formally Ni(0) center.

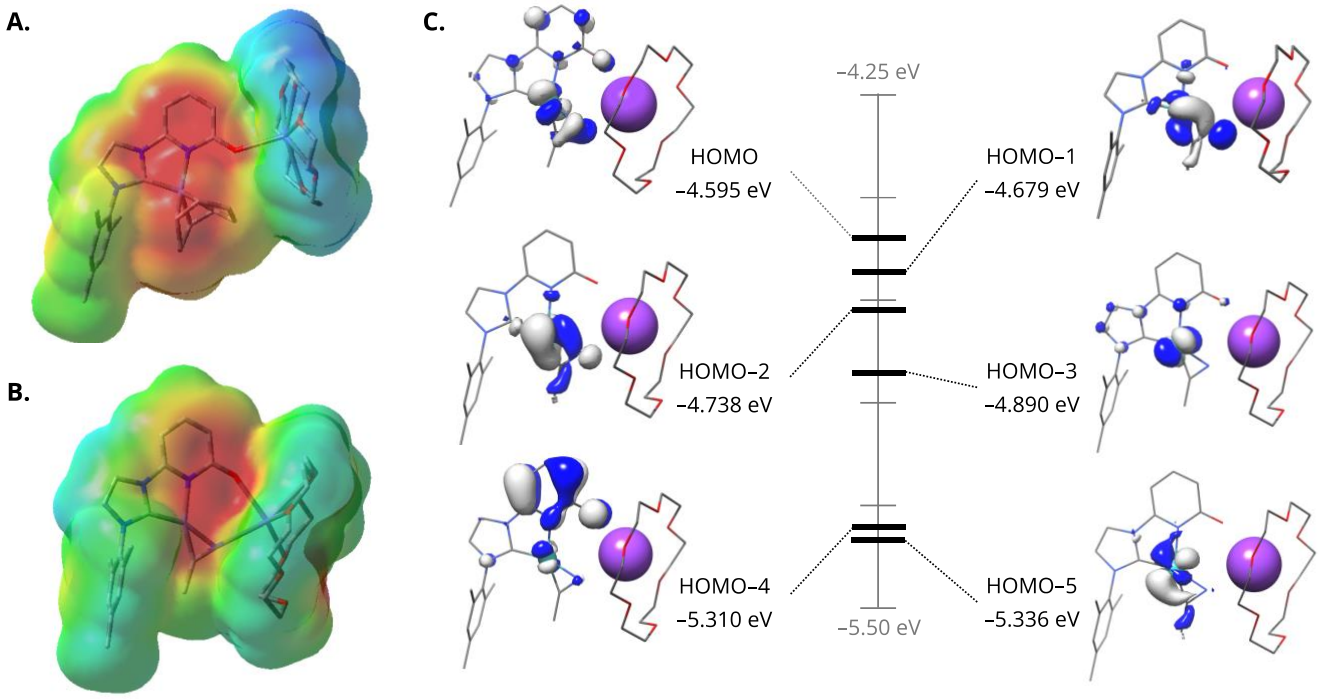

Figure 4. (A/B.) Electrostatic potential surfaces mapped onto the solid-state coordinates of **4a** and **5a**. Generated at the B3LYP/def2tzvp/SMD(THF) level of theory. Isosurfaces depicted at –0.05 (red) to +0.05 eV (blue). (C.) Computed d-orbital-like splitting diagram for 5a. Generated at the B3LYP/def2tzvp/SMD(THF) level of theory. Molecular orbital isosurfaces depicted at –0.04 (blue) to +0.05 eV (gray).

Hydroboration of Styrene. Nickel-catalyzed hydroboration of alkenes is an attractive protocol to access alkylboron compounds using either borane derivatives such as HBpin or a combination of diboron reagent such as B_2pin_2 and a proton source.[8, 48-54] Nickel-NHC complexes have been shown to catalyze hydroboration of vinyl arenes using HBpin to access branched and/or linear alkylboronate esters.[8, 48] Given this precedent, we selected hydroboration of styrene as a benchmark reaction to evaluate the catalytic activity of the (C,N)Ni complexes identified above.

Scheme 4. Nickel-Catalyzed Hydroboration of Styrene

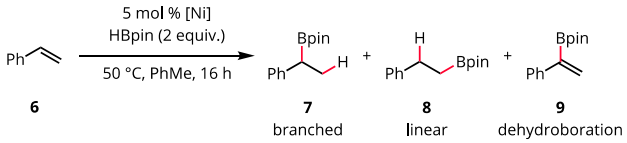

entry	[Ni]	conv. **6** [a] (yield **7**) [b]	product ratio [a] **7 : 8 : 9**
1	**4a**	≥99% (75%)	98 : 2 : 0
2	**4b**	≥99% (87%)	99 : 1 : 0
3	**4c**	≥99% (73%)	99 : 1 : 0
4	**5c**	≥99% (70%)	99 : 1 : 0
5	**4d**	60% (3%)	31 : 46 : 23

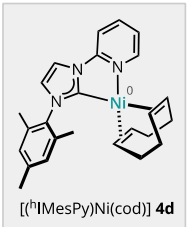

[(hIMesPy)Ni(cod)] **4d**

[a] Calculated by Gas Chromatography using dodecane as an internal standard. [b] Determined by ^{1}H NMR spectroscopy using dibromomethane as an internal standard

Combining **4a** with excess styrene (**6**) and HBpin in arene solvent (benzene-d_6 or toluene) at room temperature resulted in an immediate color change from dahlia purple to bronze and complete consumption of **4a** as detected by ^{1}H NMR spectroscopy. Although formation of hydroboration products **7** or **8** was not observed at room temperature (~25 °C), subsequent heating to 50 °C afforded a further color change of the reaction mixture to mahogany red and clean formation of branched hydroboration product **7**. Based on these observations, catalytic screening reactions were conducted with 5 mol% [Ni] in toluene at 50 °C for 16 hours (Scheme 4). Under these conditions, nickel precatalysts **4a**-**4c** and **5a** performed similarly, affording hydroboration product **7** in >70% analytical yield with excellent chemo- and regioselectivity (99:1 branched:linear; Scheme 4, entries 1–4). Negligible amounts of dehydroboration product **9** were detected.

To investigate the impact of the pyridone moiety on the yield and selectivity of the reaction, we next examined the reactivity of the analogous NHC-pyridine complex, [(hIMesPy)Ni(cod)] (**4d**).[25] When the model reaction was conducted using 5 mol % **4d** as the precatalyst, the reaction was sluggish and poorly selective. After 16 hours, the reaction reached 60% conversion of styrene, affording the hydroboration products in 3% analytical yield with a 31:46:23 **7** : **8** : **9** product ratio (Scheme 4, entry 6). These inferior results indicate that the ligand pyridone moiety plays a direct role in supporting hydroboration reactivity and selectivity.

Stoichiometric Experiments to Inform Mechanism. Based on the significance of the pyridone motif observed in hydroboration catalysis, we hypothesized that secondary Lewis acid–base interactions between HBpin and the ligand pyridone O may facilitate regioselective hydride delivery at

the β-carbon. To test the feasibility of the proposed interaction, a series of stoichiometric experiments were performed. Mixing complex **4a** with styrene (1 equiv) in C_6D_6 (Scheme 5A) did not induce any visible changes; the dahlia purple color solution persisted indefinitely at room temperature with only minor loss of the (cod) ligand as monitored by ^{1}H NMR spectroscopy. These observations indicate a low equilibrium contribution of the styrene-coordinated complex in the absence of other reagents.

Independently, complex **4c** was mixed with HBpin (1 equiv) in C_6D_6. Immediate disappearance of diagnostic HBpin resonances in the ^{1}H NMR spectrum was noted with slower consumption of **4c** over 25 hours to yield free cyclooctadiene and at least one new, desymmetrized (C,N)-ligand-containing species. To support analysis of this reaction outcome, an analogous experiment was performed using $B(OMe)_3$ as a non-hydridic, moderately Lewis acidic, C_{3h} symmetric analog of HBpin.

Scheme 5. Stoichiometric mechanistic experiments.

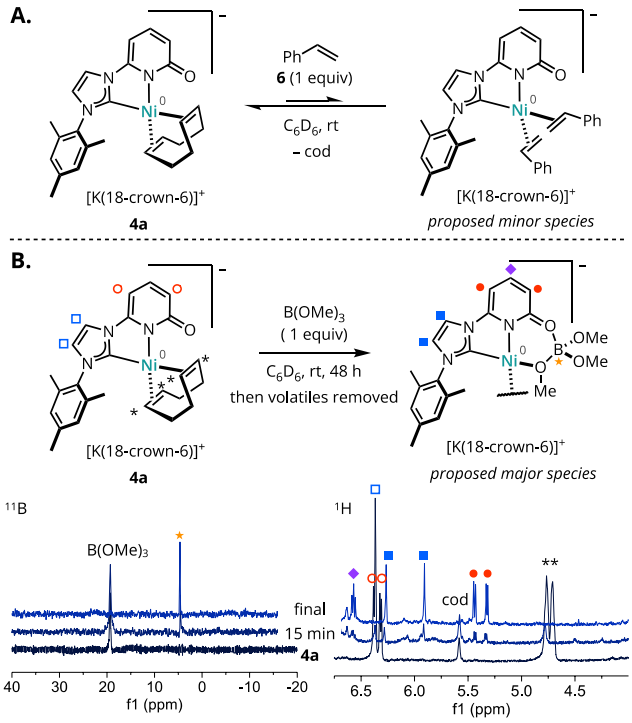

Monitoring the combination of **4a** and $B(OMe)_3$ (1 equiv) in C_6D_6 (Scheme 5B) by ^{11}B NMR spectroscopy revealed immediate appearance of a new signal at 4.6 ppm (vs. 19.3 ppm for $B(OMe)_3$), suggestive of tetravalent [B].[55] Analysis of the same sample by ^{1}H NMR spectroscopy revealed exchange-induced line broadening with gradual convergence to a new species over 48 hours. This new species, **10**, was isolated following removal of volatile components; however, attempts to obtain single-crystals suitable for X-ray diffraction were unsuccessful. Nonetheless, several distinguishing features were noted: (a) all pyridone ^{1}H NMR resonances were shifted upfield by nearly 1 ppm relative to **4a**; (b) one methyl signal (attributed to $B(OMe)_3$) showed a desymmetrized set of signals in a 2:1 ratio.; (c) none of the original signals attributed to bound cod could be resolved. On the basis of these observations, a structure involving chelation of pyridone-coordinated $B(OMe)_3$ is proposed (Figure 5B); however, the identity of any additional ligands remains unresolved. We propose that an analogous chelate involving HBpin may be responsible for the observed hydroboration catalysis.

CONCLUSION

Herein we disclosed a family of anionic, formally nickel(0) complexes supported by NHC-pyridone ligands. This ligand design supports exclusive κ^2-C,N coordination to [Ni]. The pyridone O is capped through a contact ion-pairing interaction with $[K(18\text{-crown-6})]^+$, thereby enabling isolation of monomeric species, in contrast to multimetallic clusters often generated with 2-pyridone ligands. These complexes present a sterically and electronically unsymmetric coordination environment and a highly electron-rich [Ni] core. Catalytic activity for styrene hydroboration and associated stoichiometric experiments provide support for secondary coordination sphere participation of the pyridone in delivery of the Lewis acidic HBpin reagent. Taken together, this work thus introduces a class of unconventional precatalysts while suggesting future opportunities to leverage secondary sphere reagent activation in additional transformations of interest.

EXPERIMENTAL SECTION

General Experimental Details. All air- and moisture-sensitive techniques were carried out using standard Schlenk technique on a high-vacuum line[56] or in an M. Braun glovebox containing an atmosphere of N_2. The glovebox was equipped with vacuum feed-throughs, a cold well, and a freezer for storing samples at –30 °C. Colors are described in comparison to the complete list of Prismacolor colored pencils.[57]

Materials. Reagents were purchased in reagent grade from commercial suppliers and used without further purification unless described otherwise. Bis(cyclooctadiene) nickel [$Ni(cod)_2$] was prepared according to a literature procedure[58] or purchased from Strem and stored at –30 °C in the glovebox. 1-Arylimidazoles were prepared according to a reported literature procedure.[59, 60] Solvents (acetonitrile, diethyl ether, *n*-pentane, tetrahydrofuran, and toluene) used for air- and moisture-sensitive manipulations were dried and deoxygenated by passage through an activated alumina column[61] and stored over activated molecular sieves. Deuterated solvents used for NMR spectroscopy of air- and moisture-sensitive compounds were stirred over sodium (C_6D_6, THF-d_8) or calcium hydride (CD_3CN) and distilled prior to storage in the glovebox. 18-Crown-6 was recrystallized from acetonitrile at –30 °C before use.

Instrumentation and Software. Proton nuclear magnetic resonance (^{1}H NMR) spectra were recorded at 25 °C on Bruker 400 or 500 Avance I spectrometer operating at 400.13 or 500.20 MHz. Proton-decoupled ^{13}C NMR spectra were recorded at 25 °C on Bruker 400 or 500 Avance I spectrometer operating at 100.25 or 125.78 MHz. All experiments were performed at the University of Rochester, Department of Chemistry, Nuclear Magnetic Resonance Facility. Chemical shifts are reported in parts per million downfield from tetramethylsilane ($SiMe_4$) and are referenced in ppm relative to the NMR solvent according to

literature values:[62] δ(^{1}H) = 7.16, δ(^{13}C) = 128.1 for C_6D_6.; δ(^{1}H) = 1.94, δ(^{13}C) = 118.3 for CD_3CN; δ(^{1}H) = 1.72, 3.58, δ(^{13}C) = 67.2, 25.3 for THF-d_8; δ(^{1}H) = 7.26, δ(^{13}C) = 77.2 for $CDCl_3$; δ(^{1}H) = 3.31, δ(^{13}C) = 49.0 for CD_3OD. ^{1}H NMR data for diamagnetic substances are reported as follows: chemical shift, (multiplicity, coupling constant in Hz, integration) where s = singlet, d = doublet, t = triplet, q = quartet, m = multiplet, and br = broad. ^{13}C NMR data for diamagnetic substances are reported as a list of chemical shifts. NMR spectra were processed using the MestReNova software suite. Low resolution mass spectra (LRMS) were recorded using an LC (Agilent Technology 1260 Infinity II)-MS (Advion Expression CMS) system. Infrared (FT-IR, ATR) spectra were recorded on a Shimadzu IR Affinity Fourier Transform Infrared Spectrophotometer. Electronic absorption measurements were recorded at room temperature in anhydrous THF in a sealed 1 cm quartz cuvette with an Agilent Cary 60 UV-Vis spectrophotometer.

General procedure for synthesis of 2a–2c. To a 100 mL pressure tube equipped with a PTFE-coated stir bar, 1-mesitylimidazole (8.9 mmol, 1.0 equiv.) and 6-chloro-2-hydroxypyridine (8.9 mmol, 1.0 equiv.) were added. The pressure vessel was flushed with N_2 and quickly sealed with a Teflon cap. The reaction mixture was stirred vigorously at 160 °C. (Note: The pressure vessel should be fully immersed in silicone oil up to the neck of the vessel to make sure the starting materials do not condense on the walls). The reaction was stopped once the reaction mixture turned solid (typically 3 days). The reaction mixture was then allowed to cool down to room temperature, transferred to a 500 mL round bottom flask using chloroform, and concentrated in vacuo to give brown-colored semi-solid material. The crude mixture was triturated overnight in dichloromethane to afford **2** as a putty beige solid.

1-(2,4,6-trimethylphenyl)-3-(6-hydroxypyridin-2-yl)-1H-imidazol-3-ium chloride (**2a**): 42% yield. **^{1}H NMR** (400 MHz, CD_3OD): δ 10.00 (s, 1H), 8.59 (s, 1H), 7.97 (d, *J* = 8.06 Hz, 1H), 7.96 (s, 1H), 7.46 (d, *J* = 8.06 Hz, 1H), 7.18 (s, 2H), 6.90 (d, *J* = 8.06 Hz, 1H), 2.39 (s, 3H), 2.16 (s, 6H). **^{13}C NMR** (101 MHz, CD_3OD): δ 165.4, 145.8, 144.0, 142.9, 137.0, 135.8, 132.5, 130.8, 126.4, 121.4, 112.5, 106.1, 21.1, 17.4**. LRMS** (ESI): Calculated for $C_{17}H_{18}N_3O^+$ ([M-Cl]$^+$): 280.1; found: 280.1.

1-(2,6-diethylphenyl)-3-(6-hydroxypyridin-2-yl)-1H-imidazol-3-ium chloride (**2b**): 67% yield. **^{1}H NMR** (400 MHz, CD_3OD): δ 10.12 (s, 1H), 8.63 (s, 1H), 8.06 (s, 1H), 7.98 (t, *J* = 8.0 Hz, 1H), 7.60 (t, *J* = 7.7 Hz, 1H), 7.48 (d, *J* = 8.0 Hz, 1H), 7.43 (d, *J* = 7.7 Hz, 2H), 6.91 (d, *J* = 8.0 Hz, 1H), 2.47 (qd, *J* = 7.6, 2.4 Hz, 4H), 1.20 (t, *J* = 7.6 Hz, 6H). **^{13}C NMR (**101 MHz, CD_3OD): δ 165.4, 145.8, 144.0, 142.1, 137.2, 133.6, 132.9, 128.6, 127.2, 121.4, 112.6, 106.2, 25.0, 15.4. **LRMS** (ESI): Calculated for $C_{18}H_{20}N_3O^+$ ([M-Cl]$^+$): 294.2; found: 294.3.

1-(2,6-diisopropylphenyl)-3-(6-hydroxypyridin-2-yl)-1H-imidazol-3-ium chloride (**2c**): 58% yield. **^{1}H NMR** (400 MHz, CD_3OD): δ 10.21 (s, 1H), 8.64 (s, 1H), 8.11 (s, 1H), 7.98 (t, *J* = 8.0 Hz, 1H), 7.66 (t, *J* = 7.8 Hz, 1H), 7.50 (d, *J* = 7.8 Hz, 2H), 7.46 (d, *J* = 8.0 Hz, 1H), 6.91 (d, *J* = 8.0 Hz, 1H), 2.49 (hept, *J* = 6.7 Hz, 2H), 1.32 – 1.21 (m, 12H). **^{13}C NMR** (101 MHz, CD_3OD): δ 165.4, 146.8, 145.8, 144.0, 137.3, 133.2, 131.9, 127.6, 125.9, 121.5, 112.6, 106.2, 29.9, 24.5, 24.3. **LRMS** (ESI): Calculated for $C_{20}H_{24}N_3O^+$ ([M-Cl]$^+$): 322.4; found: 322.4.

Synthesis of 3a. In an N_2-filled glovebox, a 250 mL round-bottom flask equipped with a PTFE-coated stir bar was charged with **2a** (500 mg, 1.58 mmol, 1.00 equiv.) and potassium tert-butoxide (355 mg, 3.16 mmol, 2.00 equiv.). Toluene (60 mL) was added to the reaction vessel, and the resulting mixture was stirred at room temperature for 1 hour. The reaction mixture was then passed through a short plug of Celite using a fritted filter (60 mL, C porosity) and a 500 mL filter flask, and eluted with THF. The filtrate was concentrated to give the potassium salt of the free carbene as a sienna brown solid (0.461 g, 1.45 mmol, 92% yield). To the crude material, 18-crown-6 (384 mg, 1.45 mmol) and THF (10 mL) were added, swirled to mix, and concentrated in vacuo to afford:

Potassium 1-(2,4,6-trimethylphenyl)-3-(6-oxidopyridin-2-yl)-1H-imidazol-2-ylidene (1,4,7,10,13,16-hexaoxacyclooctadecane) (**3a**). **^{1}H NMR** (400 MHz, C_6D_6): δ 8.64 (app. br s, 1H), 7.80 (d, *J* = 6.9 Hz, 1H), 7.47 (dd, *J* = 7.9, 6.9 Hz, 1H), 6.86 (s, 2H), 6.62 (d, *J* = 7.9 Hz, 1H), 6.59 (app. br s, 1H), 3.40 (s, 24H), 2.19 (s, 9H). **^{13}C NMR** (126 MHz, C_6D_6): δ 217.6, 174.2, 153.8, 140.0, 138.5, 137.0, 135.6, 129.1, 119.2, 118.3, 112.6, 94.7, 70.0, 21.3, 18.1.

General procedure for synthesis of 3b and 3c. In an N_2-filled glovebox, a 100 mL round-bottom flask was charged with **2b** or **2c** (1.12 mmol, 1.00 equiv.), a PTFE-coated magnetic stir bar, and toluene (20 mL). Potassium tert-butoxide (251 mg, 2.24 mmol, 2.00 equiv.) was weighed out into a separate vial and suspended in 15 mL toluene. The resulting KO^{t}Bu solution was added slowly to the round bottom flask while stirring vigorously at room temperature. Another 10 mL toluene was used to transfer remaining residual KO^{t}Bu to the reaction flask. The reaction mixture was stirred for 5 min after the addition of the base was complete. The reaction mixture was then passed through a short plug of celite using fritted filter (30 mL, M porosity) and a 250 mL filter flask, and eluted with THF. The filtrate was then concentrated to give the potassium salt of the free carbene as a sienna brown solid. For NMR analysis, 18-crown-6 (275 mg, 1.04 mmol) was added to the reaction vial followed by toluene (10 mL), swirled, and concentrated in vacuo to obtain:

Potassium 1-(2,6-diethylphenyl)-3-(6-oxidopyridin-2-yl)-1H-imidazol-2-ylidene (1,4,7,10,13,16-hexaoxacyclooctadecane) (**3b**). 98% yield. **^{1}H NMR** (500 MHz, C_6D_6): δ 8.86 (app. bs, 1H), 7.78 (d, *J* = 7.3 Hz, 1H), 7.45 (t, *J* = 7.3 Hz, 1H), 7.23 (t, *J* = 7.8 Hz, 1H), 7.12 (d, *J* = 7.8 Hz, 2H), 6.70 (app bs, 1H), 6.54 (d, *J* = 8.2 Hz, 1H), 3.37 (s, 24H), 2.54 (q, *J* = 7.6 Hz, 4H), 1.15 (t, *J* = 7.6 Hz, 6H). **^{13}C NMR** (128 MHz, C_6D_6): δ 217.8, 174.1, 153.8, 141.9, 141.2, 138.5, 126.7, 120.2, 118.3, 112.5, 94.8, 70.1, 66.6, 25.1, 15.6.

Potassium 1-(2,6-diisopropylphenyl)-3-(6-oxidopyridin-2-yl)-1H-imidazol-2-ylidene (1,4,7,10,13,16-hexaoxacyclooctadecane) (**3c**). 93% yield. **^{1}H NMR** (500 MHz, C_6D_6): δ 8.89 (app. br s, 1H), 7.80 (d, *J* = 7.8 Hz, 1H), 7.46 (t, *J* = 7.7 Hz, 1H), 7.33 (t, *J* = 7.7 Hz, 1H), 7.23 (d, *J* = 7.7 Hz, 2H), 6.80 (app. br s, 1H), 6.57 (d, *J* = 7.8 Hz, 1H), 3.33 (s, 24H), 3.00 (hept, *J* = 7.0 Hz, 2H), 1.27 (d, *J* = 7.0 Hz, 6H), 1.15 (d, *J* = 7.0 Hz, 6H). **^{13}C NMR** (128 MHz, C_6D_6): δ 218.2, 174.0, 154.0, 146.4, 139.8, 138.6, 123.7, 121.1, 118.6, 112.3, 95.3, 70.1, 66.9, 28.5, 24.7, 24.2.

Synthesis of nickel complexes 4a and 5a. In an N_2-filled glovebox, [Ni(cod)$_2$] (220 mg, 0.800 mmol, 0.500 equiv.) was weighed into a scintillation vial and suspended in toluene (12 mL, prechilled at –30 °C). In a 250 mL round-bottom flask, **3a** (500 mg, 1.60 mmol, 1.0 equiv.) was resuspended in toluene (50 mL, prechilled at –30 °C). The yellow [Ni(cod)$_2$] solution in toluene was added to the reaction flask while stirring vigorously at room temperature. The pale brown ligand solution turned immediately to dahlia purple. Additional toluene (20 mL, prechilled at –30 °C) was used to transfer the remaining residual [Ni(cod)$_2$] in the vial to the reaction flask. The resulting dahlia purple-colored solution was stirred at room temperature for 30 min. The crude reaction mixture was then concentrated in vacuo. The purple-colored solid was resuspended in 25 mL toluene and filtered through a pre-packed short-plug of celite (approx. 1.5 cm) using a fritted filter (60 mL, M porosity) and 500 mL filter flask to give dark red-colored solution. Another 35 mL toluene was used to transfer the crude reaction mixture onto the celite. The dark red-colored solution was discarded. The purple-colored solid left on top of the celite was then rinsed with THF (approximately 60 mL) followed by toluene (approximately 20 mL) until dahlia purple-colored solution stopped eluting. The dahlia purple-colored solution was then concentrated in vacuo to obtain **4a** as a black cherry-colored solid in 84% yield (503 mg, 0.672 mmol). Note: Excess 18-crown-6 can be removed by washing the black cherry-colored solid with 3:2 ether/pentane solution multiple times. To obtain single crystals suitable for SC-XRD, **4a** was dissolved in a minimum amount of diethyl ether and stored at –30 °C. **^{1}H NMR** (500 MHz, THF-d_8): δ 7.46 (d, J = 2.1 Hz, 1H), 6.96 (s, 2H), 6.94 (t, J = 7.7 Hz, 1H), 6.74 (d, J = 2.1 Hz, 1H), 5.99 (d, J = 7.7 Hz, 1H), 5.91 (d, J = 7.7 Hz, 1H), 3.95–3.84 (m, 4H), 3.85 (s, 24H), 2.87–2.84 (m, 2H), 2.33 (s, 3H), 2.15 (s, 6H), 1.79–1.77 (m, 2H), 1.37–1.30 (m, 4H). **^{13}C NMR** (128 MHz, THF-d_8): δ 202.3, 174.6, 148.9, 140.3, 137.7, 133.1, 129.2, 129.1, 121.8, 113.0, 108.2, 88.3, 74.1, 73.5, 71.1, 33.8, 31.7, 21.4, 18.5.

In an N_2-filled glovebox, acetonitrile (3.0 mL) was passed through a short plug of activated alumina and added to the vial containing black cherry-colored nickel complex **4a** (166 mg, 0.222 mmol). The mixture was swirled to obtain a raspberry-colored solution and then the volatiles were removed in vacuo. This procedure was repeated twice to obtain **5a** as a crimson lake-colored solid in 92% yield (139 mg, 0.204 mmol). To obtain single crystals suitable for SC-XRD, **5a** was dissolved in a minimum amount of benzene, layered with diethyl ether and stored at –30 °C. **^{1}H NMR** (400 MHz, C_6D_6): δ 7.36 (t, J = 7.7 Hz, 1H), 6.87 (s, 2H), 6.83 (app. br s, 1H), 6.70 (d, J = 7.7 Hz, 1H), 6.17 (app. br s, 1H), 5.93 (d, J = 7.7 Hz, 1H), 3.38 (s, 24 H), 2.20 (s, 6H), 2.18 (s, 3H), 1.87 (S, 3H). **^{13}C NMR** (101 MHz, C_6D_6): δ 200.2, 172.1, 167.1, 152.7, 139.0, 137.5, 136.3, 136.2, 128.3, 121.2, 114.0, 113.7, 88.0, 70.4, 21.1, 18.5, 11.8.

Synthesis of nickel complexes 4b and 5b. In an N_2-filled glovebox, [Ni(cod)$_2$] (92.8 mg, 0.0337 mmol, 0.55 equiv.) was weighed into a scintillation vial and suspended in toluene (7.5 mL, prechilled at –30 °C). In a separate vial, **3b** was suspended in toluene (5 mL, prechilled at –30 °C). The yellow-colored suspension of [Ni(cod)$_2$] in toluene was added in portions to the sample of **3b** while stirring vigorously. The pale brown solution of **3b** turned to dark purple immediately. The vial was rinsed with additional toluene (10.0 mL, prechilled at –30 °C) to quantitate the transfer of [Ni(cod)$_2$]. The resulting dark purple-colored solution was stirred at room temperature for 45 min. The crude reaction mixture was then concentrated in vacuo. The crude reaction mixture was then dissolved in THF (12 mL) and pentane (48 mL) was added slowly along the walls of the flask to precipitate a black cherry-colored solid. The THF/pentane solution was decanted, and the black cherry-colored solid in the round bottom flask was dried in vacuo to afford **4b** as a black grape-colored solid in 83% yield (225 mg, 0.280 mmol). For analytically pure material, another precipitation of **4b** from a THF solution with pentane can be carried out. To obtain single crystals suitable for SC-XRD, **4b** was dissolved in the minimum amount of diethyl ether and stored at –30 °C. **^{1}H NMR** (500 MHz, THF-d_8): δ 7.42 (app. br s, 1H), 7.27 (t, J = 7.8 Hz, 1H), 7.17 (d, J = 7.8 Hz, 2H), 6.91 (t, J = 7.8 Hz, 1H), 6.80 (app. br s, 1H), 5.96 (d, J = 7.9 Hz, 1H), 5.88 (d, J = 7.9 Hz, 1H), 3.85 (app. br s, 4H), 3.55 (s, 24H), 2.83 (br s, 2H), 2.64 (dq, J = 15.0, 8.1 Hz, 2H), 2.55 (dq, J = 15.0, 8.1 Hz, 2H), 1.82–1.61 (m, 6H), 1.11 (t, J = 7.6 Hz, 6H). **^{13}C NMR** (128 MHz, THF-d_8): δ 202.4, 174.6, 148.8, 143.8, 141.8, 133.1, 126.4, 122.9, 112.5, 108.1, 88.3, 74.3, 73.6, 71.1, 68.4, 33.8, 31.6, 26.6, 15.2.

In an N_2-filled glovebox, acetonitrile (2.0 mL) was passed through a short plug of activated alumina and added to the vial containing black cherry-colored nickel complex **4b** (22.5 mg, 0.0310 mmol). The mixture was swirled to obtain a raspberry-colored solution and then the volatiles were removed in vacuo. This procedure was repeated twice to obtain **5b** as a carmine red-colored solid in 99% yield (19.5 mg, 0.0307 mmol). **^{1}H NMR** (400 MHz, CD_3CN): δ 7.52 (d, J = 2.2 Hz, 1H), 7.39 (dd, J = 7.7, 7.8 Hz, 1H), 7.27 (d, J = 7.7 Hz, 2H), 7.21 (t, J = 7.7 Hz, 1H), 6.99 (d, J = 2.2 Hz, 1H), 6.16 (d, J = 7.7 Hz, 1H), 6.09 (d, J = 7.8 Hz, 1H), 3.53 (s, 24H), 2.49 (ddt, J = 18.8, 14.5, 7.6 Hz, 4H), 1.14 (t, J = 7.6 Hz, 6H). **^{13}C NMR** (101 MHz, CD_3CN): δ 200.1, 172.3, 152.9, 142.9, 140.3, 137.4, 129.6, 127.4, 124.5, 114.7, 114.2, 89.5, 70.7, 68.3, 26.2, 25.4, 15.5.

Synthesis of nickel complexes 4c and 5c. In an N_2-filled glovebox, [Ni(cod)$_2$] (170 mg, 0.618 mmol, 0.550 equiv.) was weighed into a scintillation vial and suspended in toluene (15 mL, prechilled at –30 °C). In a 100 mL round-bottom flask, **3c** (1.36 mmol, 1.0 equiv.) was resuspended in toluene (20 mL, prechilled at –30 °C). The yellow [Ni(cod)$_2$] solution in toluene was added to the reaction flask while stirring vigorously at room temperature. The pale brown ligand solution turned immediately to dark purple. Additional toluene (20 mL, prechilled at –30 °C) was used to transfer the remaining residual [Ni(cod)$_2$] in the vial to the reaction flask. The resulting dark purple-colored solution was stirred at room temperature for 45 min. The crude reaction mixture was then concentrated in vacuo. The crude reaction mixture was then dissolved in 14 mL THF and pentane (56 mL) was added slowly along the walls of the flask to precipitate a black cherry-colored solid. The THF/pentane solution was decanted, and the black cherry-colored solid in the round bottom flask was dried in vacuo to give **4c** in 84% yield (410 mg, 0.519 mmol). For analytically pure material, another precipitation of **4c** from a THF solution with pentane can be carried out. **^{1}H NMR**

(400 MHz, THF-d_8): δ 7.43 (s, 1H), 7.37 (t, J = 7.8 Hz, 1H), 7.26 – 7.24 (m, 2H), 6.95 (dd, J = 8.3, 7.4 Hz, 1H), 6.87 (s, 1H), 6.00 (d, J = 7.4 Hz, 1H), 5.93 (d, J = 8.3 Hz, 1H), 4.09 – 4.05 (m, 2H), 3.94 – 3.92 (m, 2H), 3.64 (s, 24H), 3.20 (sept, J = 6.8 Hz, 2H), 2.92 – 2.88 (m, 2H), 1.73 – 1.69 (m, 2H), 1.30 (d, J = 6.8 Hz, 6H), 1.29 – 1.23 (m, 4H), 1.07 (d, J = 6.8 Hz, 6H). **^{13}C NMR** (101 MHz, THF-d_8): δ 202.3, 201.5, 174.7, 148.7, 148.2, 140.7, 133.1, 129.2, 129.1, 124.7, 123.7, 112.0, 107.8, 88.3, 74.3, 72.7, 71.1, 33.7, 31.7, 29.0, 27.0, 22.5.

In an N_2-filled glovebox, acetonitrile (2.0 mL) was passed through a short plug of activated alumina and added to the vial containing black cherry-colored nickel complex **4c** (27.7 mg, 0.035 mmol). The mixture was swirled to obtain a raspberry-colored solution and then the volatiles were removed in vacuo. This procedure was repeated twice to obtain **5c** as a carmine red-colored solid in 99% yield (25.3 mg, 0.035 mmol). **^{1}H NMR** (400 MHz, C_6D_6): δ 7.36–7.28 (m, 2H), 7.21 (d, J = 7.5 Hz, 2H), 6.82 (s, 1H), 6.70 (d, J = 8.4 Hz, 1H), 6.37 (s, 1H), 5.92 (d, J = 7.0 Hz, 1H), 3.36 (s, 24H), 3.00 (sept, J = 6.8 Hz, 2H), 1.72 (s, 3H), 1.38 (d, J = 6.8 Hz, 6H), 1.13 (d, J = 6.8 Hz, 6H). **^{13}C NMR** (101 MHz, CD_3CN): δ 200.6, 172.9, 154.7, 152.8, 147.5, 138.9, 137.4, 129.9, 124.6, 124.4, 114.6, 113.9, 89.3, 70.8, 29.1, 24.2, 24.1.

General Procedure for Hydroboration of Styrene. In an N_2-filled glovebox, a 1-dram via equipped with a PTFE coated stir bar was charged with nickel complex **4** or **5** (0.010 mmol, 5 mol %). Toluene (2.0 mL) was then added, followed by styrene (23.0 μL, 0.200 mmol, 1.00 equiv.) and HBpin (58.0 μL, 0.400 mmol, 2.00 equiv.). The vial was then capped and sealed with electrical tape, removed from the glovebox, and stirred at 50 °C for 16 h. The vial was then opened to air, and an aliquot was removed for gas chromatographic analysis. The crude reaction mixture was passed through silica and eluted with 5:95 ethyl acetate/hexane. The filtrate was concentrated in vacuo and then dissolved in $CDCl_3$. The reaction was analyzed by ^{1}H NMR spectroscopy using dibromomethane (7.00 μL, 0.100 mmol) as an internal standard.[63]

ASSOCIATED CONTENT

Supporting Information

The Supporting Information is available free of charge on the ACS Publications website.

Experimental details, compound characterization data, computational methods, and results (PDF)

Crystallographic data for **4a** (CCDC 2202651), **4b** (CCDC 2202653), and **5a** (CCDC 2202652) (CIF)

AUTHOR INFORMATION

Corresponding Author

C. Rose Kennedy — Department of Chemistry, University of Rochester, Rochester, New York 14627; orcid.org/0000-0003-3681-819X Email: c.r.kennedy@rochester.edu

Authors

Medina Afandiyeva — Department of Chemistry, University of Rochester, Rochester, New York 14627; orcid.org/0000-0003-4454-5996

Abhishek A. Kadam — Department of Chemistry, University of Rochester, Rochester, New York 14627; orcid.org/0000-0001-9453-2996

Xijue Wu — Department of Chemistry, University of Rochester, Rochester, New York 14627; orcid.org/0000-0002-7840-2814

William W. Brennessel — Department of Chemistry, University of Rochester, Rochester, New York 14627; orcid.org/0000-0001-5461-1825

Author Contributions

† Authors M. A., A. A. K., and X. W. contributed equally. Although listed order is alphabetical by last name, all three are entitled to list their own name first on publication lists.

Notes

The authors declare no competing financial interest.

ACKNOWLEDGMENT

Financial support was provided by the University of Rochester. X.W. acknowledges the University of Rochester Discover Grant for a research fellowship. The authors thank Prof. Ellen Matson and Mamta Dagar (University of Rochester) for assistance with UV/vis measurements. The authors thank Ray Teng (University of Rochester) for technical assistance and Dr. Tessa Baker (University of Rochester) for guidance with NMR spectroscopy. Computations were performed on the Center for Integrated Research Computing (CIRC) BlueHive cluster at the University of Rochester

REFERENCES

1. Schmidt, A.; Wiechmann, S.; Otto, C. F., Chapter Six - N-Heterocyclic Carbenes. In *Advances in Heterocyclic Chemistry*, Scriven, E. F. V.; Ramsden, C. A., Eds. Academic Press: 2016; Vol. 119, pp 143-172.
2. Hopkinson, M. N.; Richter, C.; Schedler, M.; Glorius, F. An overview of N-heterocyclic carbenes. *Nature* **2014**, *510*, 485-496. DOI: 10.1038/nature13384
3. Prakasham, A. P.; Ghosh, P. Nickel N-heterocyclic carbene complexes and their utility in homogeneous catalysis. *Inorg. Chim. Acta* **2015**, *431*, 61–100. DOI: 10.1016/j.ica.2014.11.005
4. Zhao, Q.; Meng, G.; Nolan, S. P.; Szostak, M. N-Heterocyclic Carbene Complexes in C–H Activation Reactions. *Chem. Rev.* **2020**, *120*, 1981–2048. DOI: 10.1021/acs.chemrev.9b00634
5. Tasker, S. Z.; Standley, E. A.; Jamison, T. F. Recent advances in homogeneous nickel catalysis. *Nature* **2014**, *509*, 299-309. DOI: 10.1038/nature13274
6. Hazari, N.; Melvin, P. R.; Beromi, M. M. Well-defined nickel and palladium precatalysts for cross-coupling. *Nat. Rev. Chem.* **2017**, *1*, 0025. DOI: 10.1038/s41570-017-0025
7. Wu, J.; Faller, J. W.; Hazari, N.; Schmeier, T. J. Stoichiometric and Catalytic Reactions of Thermally Stable Nickel(0) NHC Complexes. *Organometallics* **2012**, *31*, 806–809. DOI: 10.1021/om300045t
8. Touney, E. E.; Van Hoveln, R.; Buttke, C. T.; Freidberg, M. D.; Guzei, I. A.; Schomaker, J. M. Heteroleptic Nickel Complexes for the Markovnikov-Selective Hydroboration of Styrenes. *Organometallics* **2016**, *35*, 3436–3439. DOI: 10.1021/acs.organomet.6b00652
9. Miller, Z. D.; Li, W.; Belderrain, T. R.; Montgomery, J. Regioselective Allene Hydrosilylation Catalyzed by N-Heterocyclic Carbene Complexes of Nickel and Palladium. *J. Am. Chem. Soc.* **2013**, *135*, 15282–15285. DOI: 10.1021/ja407749w
10. Nett, A. J.; Cañellas, S.; Higuchi, Y.; Robo, M. T.; Kochkodan, J. M.; Haynes, M. T.; Kampf, J. W.; Montgomery, J. Stable, Well-Defined Nickel(0) Catalysts for Catalytic C–C and C–N

Bond Formation. *ACS Catal.* **2018**, *8*, 6606–6611. DOI: 10.1021/acscatal.8b02187
11. Dander, J. E.; Garg, N. K. Breaking Amides using Nickel Catalysis. *ACS Catal.* **2017**, *7*, 1413–1423. DOI: 10.1021/acscatal.6b03277
12. van Vuuren, E.; Malan, F. P.; Landman, M. Multidentate NHC complexes of group IX metals featuring carbon-based tethers: Synthesis and applications. *Coord. Chem. Rev.* **2021**, *430*, 213731. DOI: 10.1016/j.ccr.2020.213731
13. Liu, L.-C.; Tzeng, Y.-H.; Hung, C.-H.; Lee, H. M. Multidentate N-Heterocyclic Carbene Complexes of Nickel and Palladium: Structural Analysis and Catalytic Application in Mizoroki–Heck Coupling Reaction. *Eur. J. Inorg. Chem.* **2020**, *2020*, 3601–3611. DOI: 10.1002/ejic.202000530
14. Charra, V.; de Frémont, P.; Braunstein, P. Multidentate N-heterocyclic carbene complexes of the 3d metals: Synthesis, structure, reactivity and catalysis. *Coord. Chem. Rev.* **2017**, *341*, 53–176. DOI: 10.1016/j.ccr.2017.03.007
15. Hale, L. V. A.; Szymczak, N. K. Hydrogen Transfer Catalysis beyond the Primary Coordination Sphere. *ACS Catal.* **2018**, *8*, 6446–6461. DOI: 10.1021/acscatal.7b04216
16. Moore, C. M.; Dahl, E. W.; Szymczak, N. K. Beyond H2: exploiting 2-hydroxypyridine as a design element from [Fe]-hydrogenase for energy-relevant catalysis. *Curr. Opin. Chem. Biol.* **2015**, *25*, 9–17. DOI: 10.1016/j.cbpa.2014.11.021
17. Hejazi, S. A.; Osman, O. I.; Alyoubi, A. O.; Aziz, S. G.; Hilal, R. H. The Thermodynamic and Kinetic Properties of 2-Hydroxypyridine/2-Pyridone Tautomerization: A Theoretical and Computational Revisit. *Int. J. Mol. Sci.* **2016**, *17*, 1893. DOI: 10.3390/ijms17111893
18. Khusnutdinova, J. R.; Milstein, D. Metal–Ligand Cooperation. *Angew. Chem. Int. Ed.* **2015**, *54*, 12236–12273. DOI: 10.1002/anie.201503873
19. Wong, M. W.; Wiberg, K. B.; Frisch, M. J. Solvent effects. 3. Tautomeric equilibria of formamide and 2-pyridone in the gas phase and solution: an ab initio SCRF study. *J. Am. Chem. Soc.* **2002**, *114*, 1645–1652. DOI: 10.1021/ja00031a017
20. Rawson, J. M.; Winpenny, R. E. P. The coordination chemistry of 2-pyridone and its derivatives. *Coord. Chem. Rev.* **1995**, *139*, 313–374. DOI: 10.1016/0010-8545(94)01117-T
21. Drover, M. W.; Love, J. A.; Schafer, L. L. 1,3-N,O-Complexes of late transition metals. Ligands with flexible bonding modes and reaction profiles. *Chem. Soc. Rev.* **2017**, *46*, 2913–2940. DOI: 10.1039/C6CS00715E
22. Blake, A. J.; Gilby, L. M.; Parsons, S.; Rawson, J. M.; Reed, D.; Solan, G. A.; Winpenny, R. E. P. Synthesis, structural characterisation and nuclear magetic resonance studies of cobalt complexes of pyridonate ligands. *J. Chem. Soc. Dalton Trans.* **1996**, 3575–3581. DOI: 10.1039/DT9960003575
23. Laruerta, P.; Latorre, J.; Sanaú, M.; Cotton, F. A.; Schwotzer, W. Synthesis of ruthenium(II) compounds with ortho-oxypyridinate ligands (hp). Crystal structure characterization of [Ru(η6-p-CH3C6H4CH(CH3)2)Cl(hp)]. *Polyhedron* **1988**, *7*, 1311–1316. DOI: 10.1016/S0277-5387(00)81229-2
24. Bhat, I. A.; Avinash, I.; Anantharaman, G. Nickel(II)- and Palladium(II)-NHC Complexes from Hydroxypyridine Functionalized C,O Chelate Type Ligands: Synthesis, Structure, and Catalytic Activity toward Kumada–Tamao–Corriu Reaction. *Organometallics* **2019**, *38*, 1699–1708. DOI: 10.1021/acs.organomet.8b00878
25. Craig, S. M.; Malyk, K. R.; Silk, E. S.; Nakamura, D. T.; Brennessel, W. W.; Kennedy, C. R. Synthesis and characterization of Ni(0) complexes supported by an unsymmetric C,N ligand. *J. Coord. Chem.* **2022**, accepted.
26. Hoshimoto, Y.; Hayashi, Y.; Suzuki, H.; Ohashi, M.; Ogoshi, S. One-Pot, Single-Step, and Gram-Scale Synthesis of Mononuclear [(η6-arene)Ni(N-heterocyclic carbene)] Complexes: Useful Precursors of the Ni0–NHC Unit. *Organometallics* **2014**, *33*, 1276–1282. DOI: 10.1021/om500088p
27. Saper, N. I.; Hartwig, J. F. Mechanistic Investigations of the Hydrogenolysis of Diaryl Ethers Catalyzed by Nickel Complexes of N-Heterocyclic Carbene Ligands. *J. Am. Chem. Soc.* **2017**, *139*, 17667–17676. DOI: 10.1021/jacs.7b10537
28. Liu, Y.; Cheng, J.; Deng, L. Three-Coordinate Formal Cobalt(0), Iron(0), and Manganese(0) Complexes with Persistent Carbene and Alkene Ligation. *Acc. Chem. Res.* **2020**, *53*, 244–254. DOI: 10.1021/acs.accounts.9b00492
29. Mindiola, D. J.; Hillhouse, G. L. Synthesis, Structure, and Reactions of a Three-Coordinate Nickel-Carbene Complex, [1,2-Bis(di-tert-butylphosphino)ethane]NiCPh2. *J. Am. Chem. Soc.* **2002**, *124*, 9976–9977. DOI: 10.1021/ja0269183
30. Tolman, C. A.; Seidel, W. C.; Gosser, L. W. Formation of three-coordinate nickel(0) complexes by phosphorus ligand dissociation from NiL4. *J. Am. Chem. Soc.* **1974**, *96*, 53–60. DOI: 10.1021/ja00808a009
31. Gosser, L. W.; Tolman, C. A. New three-coordinate complex of nickel(0). Tris(tri-o-tolyl phosphite)nickel. *Inorganic Chemistry* **1970**, *9*, 2350-2353. DOI: 10.1021/ic50092a030
32. Falivene, L.; Cao, Z.; Petta, A.; Serra, L.; Poater, A.; Oliva, R.; Scarano, V.; Cavallo, L. Towards the online computer-aided design of catalytic pockets. *Nat. Chem.* **2019**, *11*, 872–879. DOI: 10.1038/s41557-019-0319-5
33. Michelin, R. A.; Mozzon, M.; Bertani, R. Reactions of transition metal-coordinated nitriles. *Coord. Chem. Rev.* **1996**, *147*, 299–338. DOI: 10.1016/0010-8545(94)01128-1
34. Garcia, J. J.; Jones, W. D. Reversible Cleavage of Carbon−Carbon Bonds in Benzonitrile Using Nickel(0). *Organometallics* **2000**, *19*, 5544–5545. DOI: 10.1021/om0008474
35. Garcia, J. J.; Brunkan, N. M.; Jones, W. D. Cleavage of Carbon−Carbon Bonds in Aromatic Nitriles Using Nickel(0). *J. Am. Chem. Soc.* **2002**, *124*, 9547–9555. DOI: 10.1021/ja0204933
36. García, J. J.; Arévalo, A.; Brunkan, N. M.; Jones, W. D. Cleavage of Carbon−Carbon Bonds in Alkyl Cyanides Using Nickel(0). *Organometallics* **2004**, *23*, 3997–4002. DOI: 10.1021/om049700t
37. Walther, D.; Schönberg, H.; Dinjus, E.; Sieler, J. Aktivierung von Kohlendioxid an Übergangsmetallzentren: Selektive Cooligomerisation mit Hexin(−3) durch das Katalysatorsystem Acetonitril/Trialkylphosphan/Nickel(0) und Struktur eines Nickel(0)-Komplexes mit side-on gebundenem Acetonitril. *J. Organomet. Chem.* **1987**, *334*, 377–388. DOI: 10.1016/0022-328X(87)80100-6
38. Stolley, R. M.; Duong, H. A.; Thomas, D. R.; Louie, J. The Discovery of [Ni(NHC)RCN]2 Species and Their Role as Cycloaddition Catalysts for the Formation of Pyridines. *J. Am. Chem. Soc.* **2012**, *134*, 15154–15162. DOI: 10.1021/ja3075924
39. Lindquist, B. A.; Corcelli, S. A. Nitrile Groups as Vibrational Probes: Calculations of the C≡N Infrared Absorption Line Shape of Acetonitrile in Water and Tetrahydrofuran. *J. Phys. Chem. B* **2008**, *112*, 6301–6303. DOI: 10.1021/jp802039e
40. Rochon, F. D.; Melanson, R.; Howard-Lock, H. E.; Lock, C. J. L.; Turner, G. The vibrational spectra, crystal and molecular structure of bis(acetonitrile)dichloroplatinum(II). *Can. J. Chem.* **1984**, *62*, 860-869. DOI: 10.1139/v84-142
41. Frisch, M. J.; Trucks, G. W.; Schlegel, H. B.; Scuseria, G. E.; Robb, M. A.; Cheeseman, J. R.; Scalmani, G.; Barone, V.; Petersson, G. A.; Nakatsuji, H.; Li, X.; Caricato, M.; Marenich, A. V.; Bloino, J.; Janesko, B. G.; Gomperts, R.; Mennucci, B.; Hratchian, H. P.; Ortiz, J. V.; Izmaylov, A. F.; Sonnenberg, J. L.; Williams-Young, D.; Ding, F.; Lipparini, F.; Egidi, F.; Goings, J.; Peng, B.; Petrone, A.; Henderson, T.; Ranasinghe, D.; Zakrzewski, V. G.; Gao, J.; Rega, N.; Zheng, G.; Liang, W.; Hada, M.; Ehara, M.; Toyota, K.; Fukuda, R.; Hasegawa, J.; Ishida, M.; Nakajima, T.; Honda, Y.; Kitao, O.; Nakai, H.; Vreven, T.; Throssell, K.; Montgomery, J., J. A. ; Peralta, J. E.; Ogliaro, F.; Bearpark, M. J.; Heyd, J. J.; Brothers, E. N.; Kudin, K. N.; Staroverov, V. N.; Keith, T. A.; Kobayashi, R.; Normand, J.; Raghavachari, K.; Rendell, A. P.; Burant, J. C.; Iyengar, S. S.; Tomasi, J.; Cossi, M.; Millam, J. M.; Klene, M.; Adamo, C.; Cammi, R.; Ochterski, J. W.; Martin, R. L.;

Morokuma, K.; Farkas, O.; Foresman, J. B.; Fox, D. J. *Gaussian 16, Revision A.03*, Gaussian, Inc.: Wallingford, CT, 2016.
42. Weigend, F. Accurate Coulomb-fitting basis sets for H to Rn. *Phys. Chem. Chem. Phys.* **2006**, *8*, 1057-1065. DOI: 10.1039/B515623H
43. Weigend, F.; Ahlrichs, R. Balanced basis sets of split valence, triple zeta valence and quadruple zeta valence quality for H to Rn: Design and assessment of accuracy. *Phys. Chem. Chem. Phys.* **2005**, *7*, 3297–3305. DOI: 10.1039/B508541A
44. Becke, A. D. Density-functional thermochemistry. III. The role of exact exchange. *J. Chem. Phys.* **1993**, *98*, 5648–5652. DOI: 10.1063/1.464913
45. Marenich, A. V.; Cramer, C. J.; Truhlar, D. G. Universal Solvation Model Based on Solute Electron Density and on a Continuum Model of the Solvent Defined by the Bulk Dielectric Constant and Atomic Surface Tensions. *J. Phys. Chem. B* **2009**, *113*, 6378–6396. DOI: 10.1021/jp810292n
46. E. D. Glendening; A. E. Reed; J. E. Carpenter; Weinhold, F. *NBO Version 3.1*.
47. Reed, A. E.; Weinstock, R. B.; Weinhold, F. Natural population analysis. *J. Chem. Phys.* **1985**, *83*, 735–746. DOI: 10.1063/1.449486
48. Fan, W.; Li, L.; Zhang, G. Branched-Selective Alkene Hydroboration Catalyzed by Earth-Abundant Metals. *J. Org. Chem.* **2019**, *84*, 5987–5996. DOI: 10.1021/acs.joc.9b00550
49. Liu, J.; Chen, J.-Y.; Jia, M.; Ming, B.; Jia, J.; Liao, R.-Z.; Tung, C.-H.; Wang, W. Ni–O Cooperation versus Nickel(II) Hydride in Catalytic Hydroboration of N-Heteroarenes. *ACS Catal.* **2019**, *9*, 3849-3857. DOI: 10.1021/acscatal.8b05136
50. Kamei, T.; Nishino, S.; Shimada, T. Ni-catalyzed hydroboration and hydrosilylation of olefins with diboron and silylborane. *Tetrahedron Lett.* **2018**, *59*, 2896–2899. DOI: 10.1016/j.tetlet.2018.06.024
51. Li, J.-F.; Wei, Z.-Z.; Wang, Y.-Q.; Ye, M. Base-free nickel-catalyzed hydroboration of simple alkenes with bis(pinacolato)diboron in an alcoholic solvent. *Green Chem.* **2017**, *19*, 4498–4502. DOI: 10.1039/C7GC02282D
52. Geri, J. B.; Szymczak, N. K. A Proton-Switchable Bifunctional Ruthenium Complex That Catalyzes Nitrile Hydroboration. *J. Am. Chem. Soc.* **2015**, *137*, 12808–12814. DOI: 10.1021/jacs.5b08406
53. Tran, H. N.; Stanley, L. M. Nickel-Catalyzed Enantioselective Hydroboration of Vinylarenes. *Org. Lett.* **2022**, *24*, 395–399. DOI: 10.1021/acs.orglett.1c04073
54. Obligacion, J. V.; Chirik, P. J. Earth-abundant transition metal catalysts for alkene hydrosilylation and hydroboration. *Nat. Rev. Chem.* **2018**, *2*, 15–34. DOI: 10.1038/s41570-018-0001-2
55. Wrackmeyer, B., Nuclear Magnetic Resonance Spectroscopy of Boron Compounds Containing Two-, Three- and Four-Coordinate Boron. In *Annual Reports on NMR Spectroscopy*, Webb, G. A., Ed. Academic Press: 1988; Vol. 20, pp 61-203.
56. Burger, B. J.; Bercaw, J. E., Vacuum Line Techniques for Handling Air-Sensitive Organometallic Compounds. In *Experimental Organometallic Chemistry*, American Chemical Society: 1987; Vol. 357, pp 79–115.
57. *Complete List of Prismacolor Colored Pencils*. https://www.jennyscrayoncollection.com/2020/04/complete-list-of-prismacolor-premier.html (accessed 2022-08-20).
58. Krysan, D. J.; Mackenzie, P. B. A new, convenient preparation of bis(1,5-cyclooctadiene)nickel(0). *J. Org. Chem.* **1990**, *55*, 4229–4230. DOI: 10.1021/jo00300a057
59. Huckaba, A. J.; Senes, A.; Aghazada, S.; Babaei, A.; Meskers, S. C. J.; Zimmermann, I.; Schouwink, P.; Gasilova, N.; Janssen, R. A. J.; Bolink, H. J.; Nazeeruddin, M. K. Bis(arylimidazole) Iridium Picolinate Emitters and Preferential Dipole Orientation in Films. *ACS Omega* **2018**, *3*, 2673–2682. DOI: 10.1021/acsomega.8b00137
60. Occhipinti, G.; Bjørsvik, H.-R.; Törnroos, K. W.; Fürstner, A.; Jensen, V. R. The First Imidazolium-Substituted Metal Alkylidene. *Organometallics* **2007**, *26*, 4383–4385. DOI: 10.1021/om700590v
61. Pangborn, A. B.; Giardello, M. A.; Grubbs, R. H.; Rosen, R. K.; Timmers, F. J. Safe and Convenient Procedure for Solvent Purification. *Organometallics* **1996**, *15*, 1518–1520. DOI: 10.1021/om9503712
62. Fulmer, G. R.; Miller, A. J. M.; Sherden, N. H.; Gottlieb, H. E.; Nudelman, A.; Stoltz, B. M.; Bercaw, J. E.; Goldberg, K. I. NMR Chemical Shifts of Trace Impurities: Common Laboratory Solvents, Organics, and Gases in Deuterated Solvents Relevant to the Organometallic Chemist. *Organometallics* **2010**, *29*, 2176-2179. DOI: 10.1021/om100106e
63. Clary, J. W.; Rettenmaier, T. J.; Snelling, R.; Bryks, W.; Banwell, J.; Wipke, W. T.; Singaram, B. Hydride as a Leaving Group in the Reaction of Pinacolborane with Halides under Ambient Grignard and Barbier Conditions. One-Pot Synthesis of Alkyl, Aryl, Heteroaryl, Vinyl, and Allyl Pinacolboronic Esters. *J. Org. Chem.* **2011**, *76*, 9602–9610. DOI: 10.1021/jo201093u